JOURNAL OF VIROLOGY, June 2005, p. 6598–6609 Vol. 79, No. 11
0022-538X/05/$08.00+0 doi:10.1128/JVI.79.11.6598–6609.2005

Vaccinia Virus Nonstructural Protein Encoded by the A11R Gene Is Required for Formation of the Virion Membrane

Wolfgang Resch, Andrea S. Weisberg, and Bernard Moss*

Laboratory of Viral Diseases, National Institute of Allergy and Infectious Diseases, National Institutes of Health, Bethesda, Maryland 20892

Received 28 October 2004/Accepted 10 December 2004

The vaccinia virus A11R gene has orthologs in all known poxvirus genomes, and the A11 protein has been previously reported to interact with the putative DNA packaging protein A32 in a yeast two-hybrid screen. Using antisera raised against A11 peptides, we show that the A11 protein was (i) expressed at late times with an apparent mass of 40 kDa, (ii) not incorporated into virus particles, (iii) phosphorylated independently of the viral F10 kinase, (iv) coimmunoprecipitated with A32, and (v) localized to the viral factory. To determine the role of the A11 protein and test whether it is indeed involved in DNA packaging, we constructed a recombinant vaccinia virus with an inducible A11R gene. This recombinant was dependent on inducer for single-cycle growth and plaque formation. In the absence of inducer, viral late proteins were produced at normal levels, but proteolytic processing and other posttranslational modifications of some proteins were inhibited, suggesting a block in virus particle assembly. Consistent with this observation, electron microscopy of cells infected in the absence of inducer showed virus factories with abnormal electron-dense viroplasms and intermediate density regions associated with membranes and containing the D13 protein. However, no viral membrane crescents, immature virions, or mature virions were produced. The requirement for nonvirion protein A11 in order to make normal viral membranes was an unexpected and exciting finding, since neither the origin of these membranes nor their mechanism of formation in the cytoplasm of infected cells is understood.

Poxviruses are double-stranded DNA viruses that replicate and assemble in the cytoplasm. The most thoroughly studied member of the family, vaccinia virus (VAC) encodes approximately 200 proteins with roles in host defense, viral transcription, genome replication, and the formation of progeny virus particles (23). The assembly of progeny virions occurs in several steps that have been characterized by electron microscopy. The first recognizable virus structures are crescent-shaped membranes that appear to be covered with spicules (10) and engulf electron-dense areas of viroplasm. The closure of such membranes results in spherical, immature virions (IV). The viral genome is inserted into the IV before it is completed and is visible as a dense nucleoid. The IV undergoes several maturation steps including the proteolytic processing of precurser proteins to give rise to the intracellular mature virion (IMV). IMV particles are typically brick-shaped and contain a membrane and a core that appears dumbbell-shaped in cross-section. Some of the IMVs become wrapped by trans-Golgi or endosomal cisternae to form intracellular enveloped virions (IEV), which can egress from cells to form cell-associated enveloped virions (CEVs) or released extracellular enveloped virions (EEVs) (reviewed in reference 31).

The origin and precise structure of the IMV membrane is as yet unclear, and electron microscopic studies have led to conflicting views (reviewed in reference 34). The classical model suggests that the IV envelope is a single unit membrane, generated by an as-yet-undefined mechanism (11, 15, 16). However, other groups have proposed that the IV and IMV membranes are composed of two tightly opposed unit membranes that are derived from the endoplasmic reticulum (ER) or a compartment between the ER and the Golgi (ERGIC) (13, 26, 32). Genetic studies have been used to dissect the steps in morphogenesis. Under nonpermissive conditions, morphogenesis of F10L, H5R, G5R, A14L, A17L, and D13R mutants is arrested prior to the formation of normal crescent membranes and IVs. In the absence of functional F10 (35, 38, 41), H5 (12), or G5 (7) proteins, no recognizable viral structures are formed. In the absence of A14, vesicles and small crescents at sites distal from the viroplasm accumulate (30, 39), whereas suppression of A17 synthesis leads to the accumulation of vesicles and tubules in close association with viroplasmic foci (27, 29, 43). The absence of D13 results in viroplasmic foci that are surrounded by sheets of irregularly shaped membranes (44). Mutants that exhibit defects in the maturation of IV into IMV, wrapping of IMV, and egress from the cell have also been described.

Here we provide the first characterization of the 318-amino-acid (aa) product of the VAC A11R open reading frame (ORF), which is conserved in all poxviruses. A11 was expressed at late times of VAC infection and was associated with the viral factories but was not incorporated into IMVs. A conditional lethal mutant was unable to form crescent membranes or IVs. A11 appears to the first late VAC nonvirion protein with an essential role in viral membrane formation.

MATERIALS AND METHODS

ORF designations. ORF designations contain a capital letter indicating the HindIII fragment that contains the ORF, a number indicating the position within the fragment, and a letter indicating the direction of transcription (indicating left [L] or right [R]). The corresponding protein is named with the capital letter and number only.

* Corresponding author. Mailing address: National Institutes of Health, 4 Center Dr., Bldg. 4, Rm. 229, Bethesda, MD 20892-0445. Phone: (301) 496-9869. Fax: (301) 480-1147. E-mail: bmoss@niaid.nih.gov.

Cells and virus strains. BS-C-1 cells were maintained in minimum essential medium with Earle salts supplemented with 2.5% fetal bovine serum, 100 U of penicillin/ml, and 100 μg of streptomycin/ml. HeLa cells were maintained in Dulbecco modified Eagle medium supplemented with 10% fetal bovine serum, 100 U of penicillin/ml, and 100 μg of streptomycin/ml. HeLa cells were used for immunofluorescence experiments since they display less severe cytopathic effects when infected with VAC than do BS-C-1 cells. The WR strain of VAC and the recombinants vT7lacOI (1) and vF10V5i (35) were propagated as described previously. vA11Ri was propagated in the presence of 25 μM isopropyl-β-D-thiogalactopyranoside (IPTG). IMV particles of the WR strain were purified by sucrose gradient centrifugation as described previously (14).

Antibodies. Rabbit antisera were raised against a peptide derived from the predicted A11 sequence (aa 18 to 29 [SEDNYPSNKNYE]) and one peptide from the A3 sequence (P4b/4b; aa 632 to 643 [QYISARHITELF]) plus a C-terminal cysteine required for coupling to keyhole limpet hemocyanin (Covance Research Products, Denver, PA). Anti-A14-C (3), anti-A17-N (3), anti-D13 (B1) (33), and anti-F10 (35) rabbit antisera were described previously. Monoclonal antibodies (MAbs) recognizing the 9-amino-acid influenza A virus hemagglutinin (HA) epitope tag (Roche, Indianapolis, IN) and the 14-aa paramyxovirus SV5 P/V protein (V5) epitope tag (Invitrogen, Carlsbad, CA) were obtained commercially as agarose bead or horseradish peroxidase conjugates. Rabbit polyclonal anti-phosphotyrosine antiserum (anti-pTyr) was purchased from Zymed Laboratories (South San Francisco, CA), and the murine anti-protein disulfide isomerase (PDI) MAb was obtained from Stressgen Biotechnologies (Victory, British Columbia, Canada).

Triton X-114 extraction of VAC-infected cells. BS-C-1 cells were infected with 3 PFU per cell of WR for 1 h and washed. After 20 h, cells were washed three times with ice-cold phosphate-buffered saline, scraped, and lysed in 2 ml of cold lysis buffer (1% Triton X-114, 10 mM Tris [pH 7.4], 150 mM NaCl, 1 mM EDTA). After incubation for 1 h on ice the lysate was cleared by centrifugation in the cold for 15 min at 10,000 × *g*. The supernatant was shifted to 37°C for 3 min and centrifuged at 10,000 × *g* for 2 min at room temperature to allow aqueous and detergent phases to separate. The aqueous phase was reextracted with 200 μl of lysis buffer, and the detergent phase was reextracted with 1.5 ml of TNE buffer (10 mM Tris [pH 7.4], 150 mM NaCl, 1 mM EDTA) before analysis.

Plasmid and recombinant VAC construction. To construct pVOTE-A11R, the A11R ORF was amplified by PCR from genomic DNA using the oligonucleotide primers 5′-ATA AAT TCC ATA TGA CGA CCG TAC CAG TGA CGG A-3′ (the NdeI site is underlined) and 5′-TTA AAT AAT TTT AAT TCG TTT AAC GAA TAT CTT G-3′, and the PCR product was cloned into the NdeI-SmaI sites of pVOTE.2 downstream of an encephalomyocarditis virus leader sequence (42). This plasmid was used to introduce the repressible copy of A11R into the HA (A56R) locus of vT7lacOI by homologous recombination by using mycophenolic acid selection as described previously (42), resulting in the intermediate virus vA11R/A11Ri. The inducible A11R copy was verified by PCR amplification and sequence analysis. The endogenous A11R ORF was replaced with the enhanced green fluorescent protein (GFP) marker gene by using homologous recombination with a linear DNA fragment containing the GFP sequence flanked by partial sequences of the A10L and A12L ORFs. This fragment was generated in three steps. First, three independent PCR amplifications were carried out to amplify the flanking regions and the GFP sequence. The upstream flanking region (containing part of A10L and the A11R promoter) was amplified with the oligonucleotide primers 5′-TCG TCA AAG CGG GGT CGA TCT TGT ATT GTT ATA TAT TGT CTA A-3′ and 5′-CTT GCT CAC CAT GGT CAC TGG TAC GGT CGT tAT TTA ATA CT-3′ (the NcoI site is underlined; the lowercase nucleotide is a mutation to remove the A11R start codon). The GFP sequence was amplified with oligonucleotide primers 5′-TaA CGA CCG TAC CAG TGA CCA TGG TGA GCA AGG GCG AGG AG-3′ (the NcoI site is underlined; the lowercase nucleotide is a mutation to remove the A11R start codon) and 5′-GGG AAT GTA TTA AAT TAC TTG TAC AGC TCG TCC ATG CCG A-3′ (the Bsp1407I site is underlined). The lower flanking region (containing part of the A12L sequence) was amplified by using the oligonucleotide primers 5′-GAG CTG TAC AAG TAA TTT AAT ACA TTC CCA TAT CCA GAC AAC-3′ (the Bsp1407I site is underlined) and 5′-TAT AAT AAG ATC AAG AAC TCA CAA AAT CCG AAT CCA AGT CCG-3′. In the second step, the PCR-amplified fragments were digested with the indicated restriction enzymes and ligated together. The third step consisted of a PCR amplification with the outmost primers using the ligation reaction as a template. The final PCR product was transfected into cells infected with vA11R/A11Ri at 0.5 PFU per cell using Lipofectamine 2000 (Invitrogen). Recombinant viruses expressing GFP were isolated by five rounds of plaque purification using an inverted fluorescence microscope. The correct site of recombination was verified by PCR analysis.

Single cycle growth experiments. BS-C-1 cells were infected with 10 PFU per cell of vA11Ri or vT7lacOI in the presence or absence of IPTG. At various times after infection, cells were harvested, and crude lysates were prepared by three freeze-thaw cycles and sonication. The cell-associated virus yield was determined by plaque formation on BS-C-1 monolayers.

In vitro transcription/translations. The A11R ORF was amplified by PCR from genomic DNA with the oligonucleotide primers 5′-AAG CCT ATC CCT AAC CCT CTC CTC GGT CTC GAT TCT ACG ACG ACC GTA CCA GTG ACG-3′ or 5′-TAC CCC TAC GAC GTG CCC GAC TAC GCC ACG ACC GTA CCA GTG ACG GA-3′ and 5′-TTT TTT TTT TTT TTT TTA AAT AAT TTT AAT TCG TTT AAC-3′. The forward primers added an in-frame V5 or HA tag sequence, respectively. In a second round of PCR amplification with the same reverse primer, the following forward primers were used to add a T7 bacteriophage promoter to the PCR products: 5′-ATG CTA ATA CGA CTC ACT ATA GGG CCG CCA CCA TGG GTA AGC CTA TCC CTA ACC CTC-3′ and 5′-TAC CCC TAC GAC GTG CCC GAC TAC GCC ACG ACC GTA CCA GTG ACG GA-3′. A11V5 and A11HA were expressed in vitro from the described PCR products according to the manufacturer's instructions (Promega, Madison, WI) and subjected to immunoprecipitation as described below.

Plasmid transfection into vA11Ri-infected cells. BS-C-1 cells were infected with 10 PFU per cell of vA11Ri for 1 h, washed, and transfected with pcDNA or pcDNA-A32HA (provided by A. Garcia) in the presence or absence of IPTG by using Lipofectamine 2000 (Invitrogen). pcDNA-A32HA expression was not affected by IPTG. After 24 h, cell extracts were prepared and subjected to immunoprecipitation.

Immunoprecipitation of proteins. Cells were lysed in phosphate- or Tris-buffered saline containing 0.5% Nonidet P-40, protease inhibitor cocktail tablets (Roche Molecular Biochemicals, Indianapolis, IN), 5% glycerol, and 2 mM EDTA for 20 min on ice, and lysates were then clarified by centrifugation at 20,000 × *g* for 30 min at 4°C. Prior to immunoprecipitation, lysates were incubated with protein G-Sepharose beads (Amersham Biosciences, Piscataway, NJ) for 1 h at 4°C. For anti-A11 precipitations, rabbit preimmune serum was included in this step. Proteins were then captured with anti-A11 bound to protein-G beads or anti-HA beads at 4°C for 2 h. Beads were washed five times with lysis buffer, and bound proteins were eluted with 2× sodium dodecyl sulfate (SDS) sample buffer (Invitrogen). Eluates were analyzed by SDS-PAGE (PAGE) and visualized by autoradiography, in the case of radioactively labeled targets, or by Western blotting and immunological detection (see above).

Western blot analysis. Proteins from infected cell lysates or immunoprecipitates were resolved by SDS-PAGE on preprepared gels (Invitrogen) and were electrophoretically transferred to nitrocellulose membranes. Nonspecific binding sites were blocked with 5% nonfat dried milk or 5% bovine serum albumin in Tris-buffered saline, and then membranes were probed with either rabbit polyclonal antisera, followed by anti-rabbit immunoglobulin G conjugated to horseradish peroxidase, or with anti-epitope tag MAbs directly conjugated to horseradish peroxidase. Bound antibody was detected by chemiluminescence with commercial reagents (Pierce, Rockford, IL).

Pulse-labeling of proteins with [^{35}S]methionine and [^{35}S]cysteine. BS-C-1 cells were infected with 5 PFU of VAC per cell for 1 h at 37°C. After adsorption, cells were washed three times and incubated at 37°C in Eagle modified essential medium supplemented with 2.5% fetal bovine serum in the presence or absence of 25 μM IPTG. At 30 min before the indicated times, the medium was replaced with cysteine- and methionine-free medium, and cells were incubated for 30 min at 37°C, followed by the addition of 100 μCi of a mixture of [^{35}S]methionine and [^{35}S]cysteine per ml of medium. After a 30-min pulse-labeling period, cells were harvested immediately, or the labeling medium was removed and replaced with regular medium for a chase period of 15 h. Harvested cells were washed once with cold phosphate-buffered saline, and whole-cell lysates were prepared in 1× sample buffer (Invitrogen). Samples were separated on 4 to 12% gradient SDS-PAGE gels with 3-(*N*-morpholino)propanesulfonic acid running buffer (Invitrogen).

Metabolic labeling of proteins with [^{32}P]orthophosphate or [^{35}S]methionine and [^{35}S]cysteine. BS-C-1 cells were infected with vA11Ri or vF10V5i as described above at 10 PFU per cell in the presence or absence of 50 μM IPTG. After 8 h the medium was replaced with phosphate-free medium containing 100 μCi of [^{32}P]orthophosphate or methionine- and cysteine-free medium containing 50 μCi of a mixture of [^{35}S]methionine and [^{35}S]cysteine per ml. Cells were incubated at 37°C for an additional 16 h, harvested, washed with cold phosphate-buffered saline, and subjected to immunoprecipitation as described above, except for the inclusion of 50 mM sodium fluoride and 0.2 mM sodium orthovanadate in all buffers to inhibit phosphatase activity.

Confocal microscopy. HeLa cells were seeded onto glass coverslips, allowed to attach overnight, and infected with vA11Ri at 5 PFU per cell in the presence or

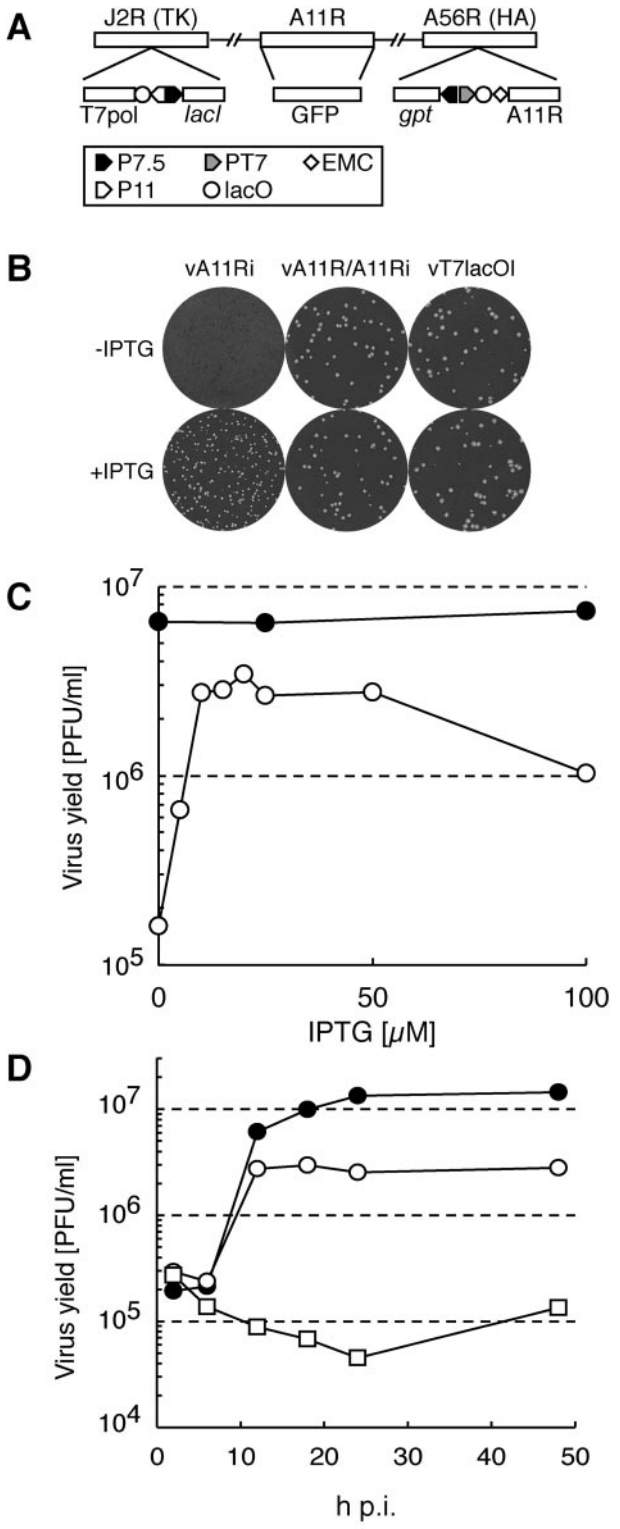

FIG. 1. Construction and characterization of a recombinant VAC with an inducible A11R ORF (vA11Ri). (A) Genome structure of vA11Ri. The three loci at which vA11Ri differs from the WR strain are shown as boxes: J2R (thymidine kinase; TK), A11R and A56R (hemagglutinin; HA). Below the boxes are schematics of the modifications. Additional abbreviations: T7pol, bacteriophage T7 RNA polymerase gene; lacO, *lac* operator; P11, a VAC late promoter; P7.5, a VAC early/late promoter; *lacI*, *E. coli lac* repressor gene; *gpt*, *E. coli* guanine phosphoribosyltransferase gene; PT7, bacteriophage T7 promoter; EMC, encephalomyocarditis virus cap-independent translation enhancer element. (B) Plaque phenotype of vA11Ri. BS-C-1 cells were infected with vA11Ri, vA11Ri/A11R and vT7lacOI in the absence or presence of 25 μM IPTG. After 48 h, the cells were fixed and stained with crystal violet. (C) Dependency of vA11Ri replication on IPTG. BS-C-1 cells were infected with 10 PFU per cell of vT7lacOI (●) or with vA11Ri (○) in the presence of 0 to 100 μM IPTG, and the viral yield was determined after 24 h. (D) One-step growth curve of vA11Ri. BS-C-1 cells were infected with 10 PFU per cell of vT7lacOI (●) or vA11Ri in the absence (□) or presence (○) of 25 μM IPTG, and the virus yield was determined from 2 to 48 h postinfection (h p.i.).

absence of 25 μM IPTG. At 8 h postinfection, cells were fixed in 4% paraformaldehyde and permeabilized with 0.2% Triton X-100, and nonspecific sites were blocked with 1% bovine serum albumin, all in phosphate-buffered saline. Coverslips were then incubated with the polyclonal anti-A11 antiserum at a 1:1,200 dilution, followed by a 1:100 dilution of a goat anti-rabbit antibody conjugated to rhodamine red (Jackson Immunoresearch Laboratories, West Grove, PA). Stained coverslips were mounted in Mowiol containing 1 μg of the DNA stain DAPI (4′,6′-diamidino-2-phenylindole; Molecular Probes, Eugene, OR)/ml. Images were acquired on a Leica TCS-NT/SP2 confocal microscope system.

Electron microscopy. BS-C-1 cells were grown in 60-mm-diameter dishes and infected with 3 PFU per cell vA11Ri or WR. vA11Ri infections were carried out in the presence or absence of 25 μM IPTG. At 20 h after infection, cells were fixed and prepared for transmission electron microscopy or immunoelectron microscopy as described previously (6, 8).

RESULTS

A11R ORF encodes an essential viral protein. To determine whether A11R was an essential gene, we generated a recombinant VAC (vA11Ri) in which A11 synthesis was dependent on the presence of an inducer. vA11Ri was constructed in two steps. First, an inducible copy of the A11R ORF was inserted into the A56R HA locus of vT7lacOI (42), itself a recombinant VAC expressing the *lac* repressor and the T7 RNA polymerase under the control of a *lac* operator (Fig. 1A). In the second step, the endogenous A11R ORF was removed from this intermediate virus (vA11R/A11Ri) and replaced with the GFP marker gene by homologous recombination to produce vA11Ri (Fig. 1A). vA11Ri was unable to produce visible plaques after 48 h in BS-C-1 cells in the absence of IPTG but produced plaques that were slightly smaller than either the intermediate or the parental virus in the presence of 25 μM IPTG (Fig. 1B).

Virus yield under single-cycle conditions increased with IPTG concentrations up to 25 μM (Fig. 1C). Note that higher concentrations of IPTG resulted in submaximal yields of vA11Ri, but not of vT7lacOI, suggesting that A11 overexpression was inhibitory. Even with the optimal IPTG concentration the yield of vA11Ri was half that of the parental strain, a finding consistent with the difference in plaque size. At 25 μM, the kinetics of virus production under single cycle conditions was similar for vA11Ri and vT7lacOI (Fig. 1D). In the absence of IPTG, vA11Ri infectivity declined over time but increased slightly between 24 and 48 h, a finding consistent with a small amount of A11 protein detected by Western blot analysis 48 h after infection (data not shown).

The A11R ORF encodes a late protein that is not present in IMV or incorporated into membranes. Sequence analysis predicted that the A11R ORF encodes a protein with a mass of 36 kDa that is expressed at late times of infection. To determine whether A11 is produced with late kinetics, whole-cell extracts

of VAC-infected cells were analyzed by SDS-PAGE and Western blotting with a rabbit antiserum raised against amino acids 18 to 29 of the predicted A11 sequence. A protein band of ca. 40 kDa was observed at 6 h after infection and continued to increase until 24 h (Fig. 2A). In the presence of cytosine arabinoside, an inhibitor of VAC DNA replication, no A11 was detected at 8 h, and only a small amount was observed at 24 h (Fig. 2). The timing of A11 synthesis and dependence on DNA replication indicated that A11 belongs to the late class of proteins. The mobility of the A11 protein was identical under reducing and nonreducing conditions, indicating that the two cysteine residues present in the protein were probably not involved in intermolecular disulfide bonding (data not shown).

Although A11 was readily detected in extracts of VAC-infected cells, the protein was undetectable in whole virions or NP-40 extracts of virions (Fig. 2B). In contrast, both a core protein (P4b/4b) and a membrane protein (A14) were detected in the cell extract and purified IMV (Fig. 2B).

Two hydrophobic regions in the A11R sequence were predicted by sequence analysis to encode putative transmembrane domains. To determine whether A11 was indeed a transmembrane protein, VAC-infected cells were extracted with Triton X-114. A11 was completely solubilized by 1% Triton X-114 in the cold, and the majority of A11 partitioned into the aqueous phase during phase separation at 37°C (Fig. 2C). The membrane protein A17, however, partitioned completely into the detergent phase. Taken together, these data indicate that A11 is not associated with virions or membranes.

A11 is phosphorylated by a largely F10-independent mechanism. The slower-than-predicted migration of A11 suggested that A11 might be a phosphoprotein. To test this possibility, cells were infected with vA11Ri in the absence or presence of 50 μM IPTG and metabolically labeled from 8 h to 24 h postinfection with either [^{32}P]orthophosphoric acid or a mixture of [^{35}S]methionine and [^{35}S]cysteine. Cytoplasmic extracts were prepared, and proteins bound by anti-A11 antiserum were resolved by SDS-PAGE (Fig. 3). ^{35}S- and ^{32}P-labeled bands of the same size as that observed in Western blots of infected cell lysates were seen only in the presence of IPTG, indicating that A11 was indeed phosphorylated. An additional lower band was detected by immunoprecipitation that was not seen in Western blots with the same antiserum raised against amino acids 18 to 29. However, antiserum raised against a peptide closer to the C terminus recognized the lower band in Western blots of proteins expressed by vA11Ri (data not shown), suggesting that this protein might form by initiation at the second ATG, which is downstream of amino acids 18 to 29. Since the shorter protein was detected in immunoprecipitations with the anti-A11 antiserum, despite the lack of the recognized peptide, it must interact with full-length A11 to form a dimer or higher oligomer (see below). Note that this short form of A11 was not found during infection with WR and is an artifact of the inducible expression system.

To test whether the phosphorylation was dependent on F10, the experiment described above was carried out with vF10V5i, a VAC recombinant with an inducible F10L gene fused to the V5 epitope tag. In this construct A11 is expressed from its natural promoter, and only the full-length protein was detected. In the absence of F10 synthesis, A11 was still phosphorylated, suggesting that there was a F10-independent phosphor-

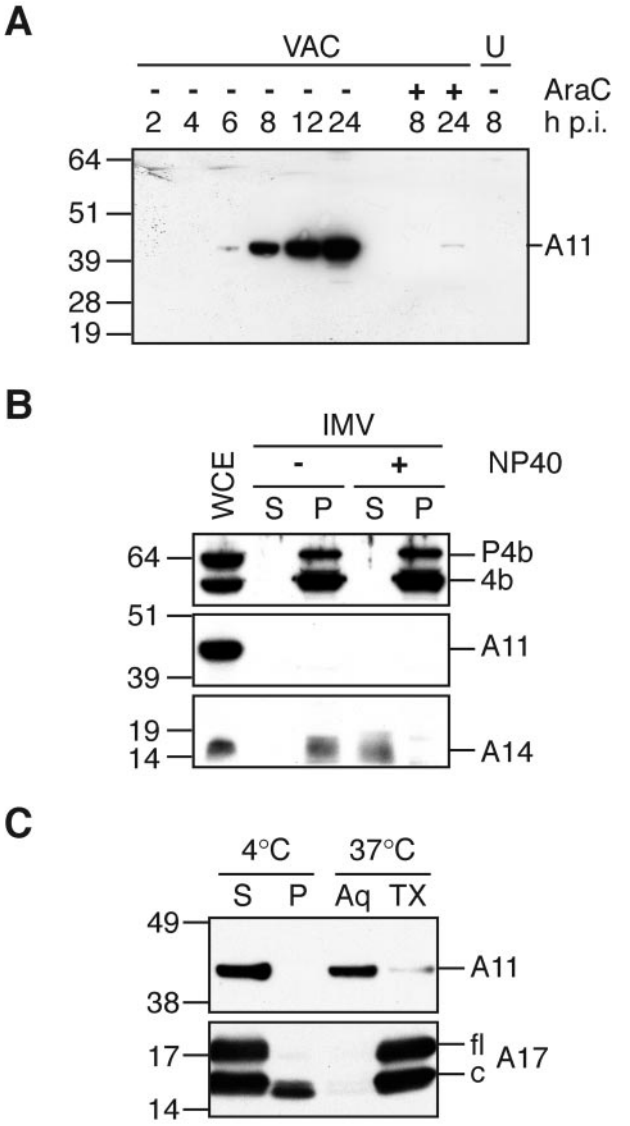

FIG. 2. Synthesis of A11 and analysis of IMV. (A) A11 expression kinetics. BS-C-1 cells were infected with 10 PFU per cell of VAC and whole-cell extracts were prepared at the indicated times. Extracts from uninfected cells (U) and cells infected in the presence of cytosine arabinoside (AraC) were also prepared, and all extracts were analyzed by SDS-PAGE and Western blotting with a anti-A11 antiserum. The position and mass in kilodaltons of marker proteins are indicated on the left. Note that the apparent molecular mass of A11 is slightly larger than predicted. (B) Absence of A11 in purified IMV. Purified IMV was extracted with NP-40 (+) or mock treated (−) and separated into soluble (S) and pellet (P) fractions. Proteins in both fractions were separated by SDS-PAGE, followed by Western blotting with anti-P4b, anti-A11, or anti-A14 antisera. Whole-cell extract (WCE) containing similar amounts of P4b/4b and A14 was included in the analysis. The position and mass in kilodaltons of marker proteins are indicated on the left. (C) Phase separation of A11 in Triton X-114. BS-C-1 cells were infected with 3 PFU per cell of VAC. After 20 h, cells were harvested in cold lysis buffer containing 1% Triton X-114. The lysate was separated into soluble (S) and pellet (P) fractions, and the soluble fraction was separated into aqueous (Aq) and detergent (TX) phases. All samples were adjusted to equal volumes and subjected to SDS-PAGE, followed by Western blotting with anti-A11 or anti-A17 antisera. The position and mass in kilodaltons of marker proteins are indicated on the left. Lines on the right point to the full-length (fl) and cleaved (c) forms of the A17 protein.

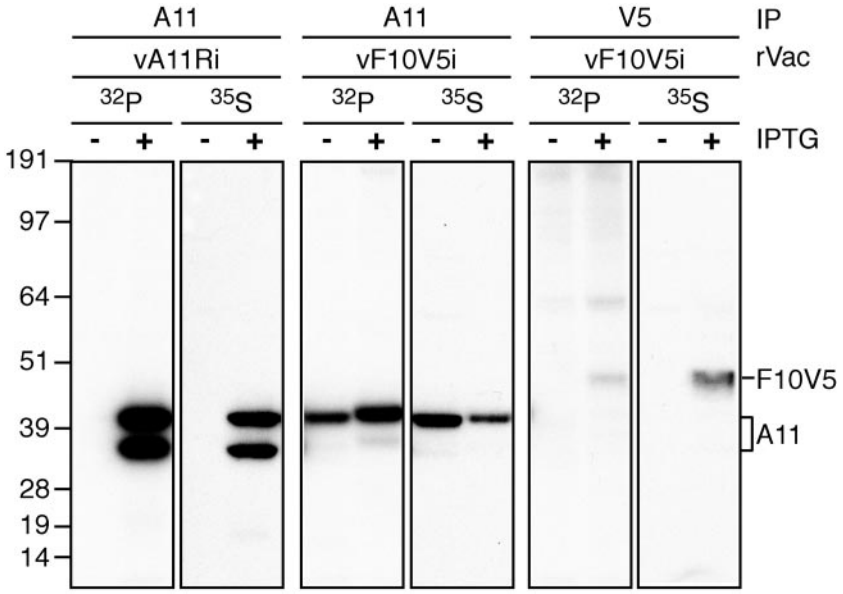

FIG. 3. Phosphorylation of A11. BS-C-1 cells were infected with 10 PFU per cell of the indicated recombinant VAC (rVAC) in the presence or absence of 50 μM IPTG. Infected cells were metabolically labeled either with a mixture of [^{35}S]methionine and [^{35}S]cysteine (^{35}S) or with [^{32}P]orthophosphate (^{32}P) from 1 h until 20 h after infection. After labeling, cytoplasmic extracts were prepared, and proteins were captured with either anti-A11 (A11) or anti-V5 (F10V5) antibodies. The antibody-bound proteins were resolved by SDS-PAGE and visualized by autoradiography. The bands corresponding to A11 and F10V5 are indicated on the right. Note that the lower band seen in immunoprecipitations from vA11Ri-infected cells represents an internal translation initiation product. Position and mass of marker proteins are shown on the left in kilodaltons.

ylation. The repression of F10V5 in the absence of IPTG was confirmed by immunoprecipitation with anti-V5 MAb from extracts prepared in parallel from vF10V5i-infected cells. Under these conditions, neither a ^{35}S-labeled protein nor the autophosphorylated form of F10V5 could be detected, suggesting that the phosphorylation of A11 did not result from leaky synthesis of F10V5. Nevertheless, in the presence of F10, there appeared to be an increase in A11 phosphorylation as indicated by band intensity and a small mobility shift. This greater phosphorylation could not be explained by increased A11 expression as detected by immunoprecipitation from ^{35}S-labeled cells.

A11 interacts with A32 and with itself. A11 was reported previously to interact with A32, a protein involved in DNA packaging (5), in a yeast two-hybrid screen (20). To confirm this interaction, BS-C-1 cells were infected with vA11Ri in the presence or absence of IPTG and then transfected with either empty vector or pcDNA-A32HA. Proteins were precipitated with anti-A11 or anti-HA antibodies from cell extracts prepared 24 h after infection. Precipitates and cell lysates were analyzed by Western blotting (Fig. 4A). As expected A11 and A32 synthesis were dependent on IPTG and transfection with pcDNA-A32HA, respectively (Fig. 4A). For unknown reasons, synthesis of A11 was reduced in A32HA transfected cells. Immunoprecipitation of either A11 or A32HA resulted in the coimmunoprecipitation of the other protein (Fig. 4A). This suggested that A11 and A32 do interact. The low level of coprecipitation, however, suggested that the majority of either protein is not involved in this complex or that the complex is not very stable. In addition, this interaction could not be detected with in vitro-synthesized proteins (data not shown).

Data presented in the previous section had suggested that A11 might interact with itself. To confirm this interaction, in vitro transcription-translation reactions were programmed with PCR products encoding A11HA and/or A11V5. Analysis of the total reaction by Western blotting indicated that both proteins were made (Fig. 4B). A11HA was captured with anti-HA antibody conjugated to agarose beads, and bound proteins were analyzed. A11V5 was detected in anti-HA immunoprecipitates only if A11HA was coexpressed (Fig. 4B), indicating that A11 interacted with itself to form dimers or higher-order complexes.

The A11 protein is localized in the viral factory. The absence of A11 from purified IMV raised the possibility that it did not localize in the factories when assembly occurs. To determine the subcellular localization of A11, we carried out immunofluorescence experiments in HeLa cells that were infected for 8 h with vA11Ri in the absence or presence of 25 μM IPTG. An IPTG-dependent signal was observed for A11 (Fig. 5) and colocalized with the cytoplasmic viral factories identified with the fluorescent DNA stain DAPI. At 12 h postinfection A11 was observed to extend slightly beyond the boundaries of the factory (data not shown). Immunoelectron microscopy confirmed the factory localization, but A11 was not specifically associated with discrete recognizable structures (data not shown).

Viral proteins are synthesized normally but processing of core proteins is inhibited in the absence of A11. VAC gene expression occurs as an ordered progression of early, intermediate and late protein synthesis. Concomitantly, host protein synthesis is reduced, allowing abundant late viral proteins to be selectively labeled with radioactive amino acids. Viral protein synthesis was analyzed by pulse-labeling BS-C-1 cells infected with vT7lacOI or vA11Ri in the presence or absence of 25 μM IPTG. Whole-cell extracts of labeled cells were subjected to SDS-PAGE and autoradiography. As seen in Fig. 6A, cellular

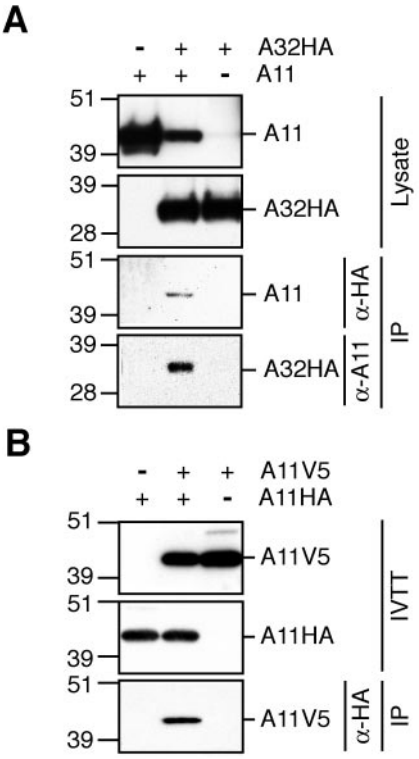

FIG. 4. Coimmunoprecipitation of A11 with A32 and itself. (A) Coimmunoprecipitation of A11 and A32HA. BS-C-1 cells were infected with 10 PFU per cell of vA11Ri in the presence (A11+) or absence (A11−) of IPTG. Cells were then transfected with either pcDNA-A32HA (A32HA+) or empty vector (A32HA−). After 24 h, cytoplasmic extracts were prepared and proteins were precipitated with either anti-HA antibody or anti-A11 antiserum bound to agarose beads. Lysate and precipitate were analyzed by Western blotting. Position and mass in kilodaltons of marker proteins are indicated on the left. (B) Coimmunoprecipitation of differently tagged forms of A11. IVTT reactions were programmed with PCR products encoding A11HA and/or A11V5. After 90 min of protein synthesis, the IVTT reactions were subjected to immunoprecipitation with anti-HA antibody bound to agarose beads and reactions, and precipitates were analyzed by Western blotting with the anti-V5 antibody directly conjugated to horseradish peroxidase.

protein synthesis largely stopped between 6 and 9 h postinfection under all three conditions. Except for some minor bands, the pattern of viral protein synthesis was similar in cells infected with vA11Ri with or without IPTG and the parental vT7lacOI.

The largely normal pattern of protein synthesis suggested that early steps in the life cycle were not dependent on A11, a finding consistent with its late expression and absence from mature virions. To determine whether virion maturation was proceeding normally in the absence of A11, we analyzed the proteolytic processing of core proteins, an obligatory step in the transition from immature to mature virus particles (2, 4, 17). To this end, cells were infected as described above, pulse-labeled 9 h later, and either harvested directly or shifted to chase medium with excess unlabeled methionine and cysteine for a further 15 h. As a control for incomplete processing of core proteins, vT7lacOI infections were also carried out in the presence of rifampin, an inhibitor of morphogenesis. Synthesized proteins and their processed products were analyzed by SDS-PAGE and autoradiography (Fig. 6B). Two major core protein precursors, P4a and P4b, were synthesized normally under all conditions. However, processing of P4a and, to a lesser degree, P4b was inhibited in cells infected with vA11Ri in the absence of IPTG and in cells infected with vT7lacOI in the presence of rifampin. IPTG relieved the processing defect in vA11Ri-infected cells, allowing the products 4a and 4b to accumulate during the chase period (Fig. 6B). These results suggested that morphogenesis was inhibited in the absence of A11.

Expression and posttranslational modification of proteins involved in early steps of morphogenesis are altered in the absence of A11. Early blocks in morphogenesis can alter the levels and posttranslational modifications of membrane proteins (12, 36). To determine whether the absence of A11 had such effects, cells were infected with vA11Ri in the presence of 0 to 100 μM IPTG, and several proteins were analyzed by SDS-PAGE and Western blotting of whole-cell extracts prepared 24 h after infection. Under these conditions, A11 was not detected at IPTG concentrations of <5 μM, and A11 levels increased progressively with increasing IPTG concentration (Fig. 7). In the absence of A11, A17 was synthesized but neither cleaved nor phosphorylated. Phosphorylation of A17 is dependent on the F10 kinase (3), which was reduced in amount when A11 was absent. In addition, as has been reported previously for other mutants with blocks in early morphogenesis (21), A14 was partially glycosylated resulting in slower mobility in vA11Ri-infected cells under nonpermissive conditions, but not under permissive conditions. The core protein precursor P4b, on the other hand, was expressed at similar levels irrespective of IPTG concentration, but the mature cleavage product 4b increased with increasing IPTG.

Morphogenesis of vA11Ri under nonpermissive conditions. To determine the exact stage at which virus morphogenesis was arrested in the absence of A11 expression, BS-C-1 cells were infected with vA11Ri in the absence or presence of 25 μM IPTG, and thin sections were examined by electron microscopy 20 h after infection. In the presence of IPTG, the cytoplasm of vA11Ri-infected cells contained the full range of normal viral structures, including viral crescents, IVs, IMVs, and enveloped virions (Fig. 8A). Without IPTG, however, morphogenesis was arrested at an early stage, before the formation of crescent membranes (Fig. 8B). Viral factories cleared of cellular organelles were present, as were areas of electron-dense viroplasm inside the factories. In addition, we observed areas of intermediate electron density that were surrounded and invaded by membranes. Figures 8C and D show higher magnifications of the membrane-surrounded structures.

The membrane-associated areas of intermediate electron density were reminiscent of D13 inclusion bodies observed in infected, rifampin-treated cells (33). We therefore used rabbit anti-D13 antiserum to localize D13 by immunoelectron microscopy in thawed cryosections of cells infected with vA11Ri in the absence of IPTG. The majority of staining was detected in the inclusion body-like structures that likely corresponded to the membrane-invaded intermediate density regions seen in Epon-embedded sections (Fig. 9A). However, a minor amount of D13 was also detected in the more electron-dense viroplasm. Under these conditions, the core protein P4b/4b was largely localized to the viroplasm, which was morphologically

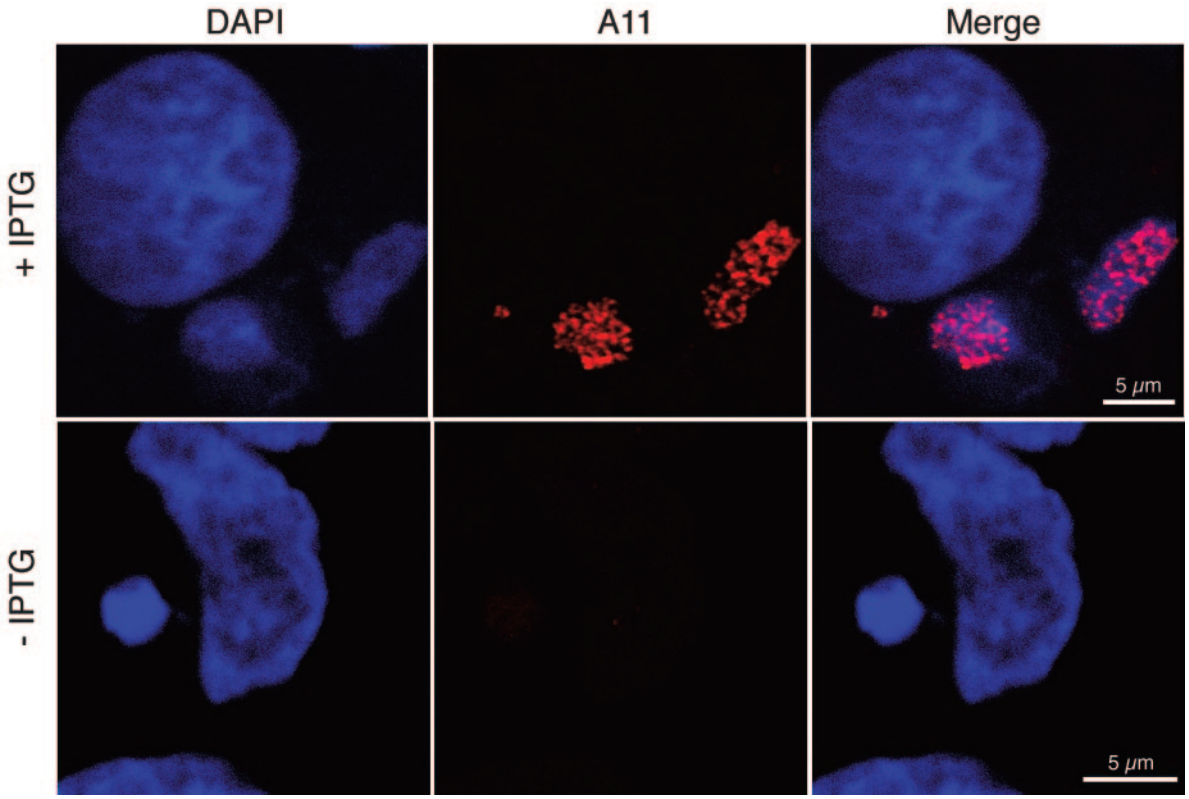

FIG. 5. Localization of A11 by confocal microscopy. HeLa cells were infected with 5 PFU per cell of vA11Ri in the presence or absence of 25 μM IPTG. After 8 h cells were fixed, permeabilized, and stained with (i) anti-A11 antiserum, followed by rhodamine red-conjugated goat anti-rabbit antibody, and (ii) the DNA stain DAPI. Shown are single optical sections with scale bars recorded by confocal microscopy. Colors: blue, DAPI (nuclei and viral factories); red, A11.

distinct from the D13 inclusions (Fig. 9B). To further characterize the membranes that were associated with the D13 inclusions, we tested for the presence of the A17 viral IMV membrane protein and the ER-resident PDI. As seen in Fig. 9C and D, light A17 and PDI staining was observed in association with the invading membranes in the intermediate density areas.

DISCUSSION

The A11R ORF is one of the 49 genes that are conserved in all sequenced poxviruses (40). The protein, however, was not previously characterized except for a report that it interacts with A32, a protein involved in DNA packaging (20). Sequence analysis revealed elements of a late promoter, as well as two putative hydrophobic trans-membrane helices, but no motifs or homologs outside the poxviruses that could provide insight into A11 function. Western blotting showed that A11 was indeed expressed late with an apparent mass of 40 kDa, slightly larger than the predicted mass of 36 kDa. A11 was not detected in purified IMV but was shown by confocal microscopy of fluorescently stained cells to be located in the viral factories. Immunoelectron microscopy confirmed the factory localization of A11 but did not reveal an association with any recognizable structures. In particular, A11 was not preferentially detected in viral membranes, suggesting that the hydrophobic segments do not function as transmembrane domains. Consistent with this observation, A11 partitioned largely into the aqueous phase during Triton X-114 extractions.

A conditional lethal mutant (vA11Ri) was generated in which A11 synthesis was suppressed in the absence of the inducer IPTG. This virus was dependent on IPTG for spread and virus production in cells infected at a high multiplicity, indicating that A11R is an essential gene. However, a low level of replication was detected after 48 h of infection in the absence of IPTG. Since all experiments presented here were completed in 24 h or less, this should not have any impact on the interpretation of our results. vA11Ri replicated to levels about half that of the parental virus at the optimal IPTG concentration of 25 μM. Higher concentrations of IPTG resulted in higher A11 expression levels and reduced virus yields, suggesting that A11 overexpression might be inhibitory.

Viral morphogenesis was interrupted at a significantly earlier stage in the absence of A11 (see below) than it was in the absence of A32 (5), suggesting that the earliest essential function of A11 is independent of A32 and DNA packaging. However, we could confirm the previously reported interaction of A11 with A32 by coimmunoprecipitation, albeit only at a low level. Together, these findings suggest that either the interaction was not physiologically relevant or A11 has more than one function.

A robust interaction was detected between two forms of A11 fused to different epitope tags coexpressed in vitro, explaining the coimmunoprecipitation of short and full-length forms of A11 in vivo. This indicated that A11 formed a higher-order complex, although the number of subunits in the complex or

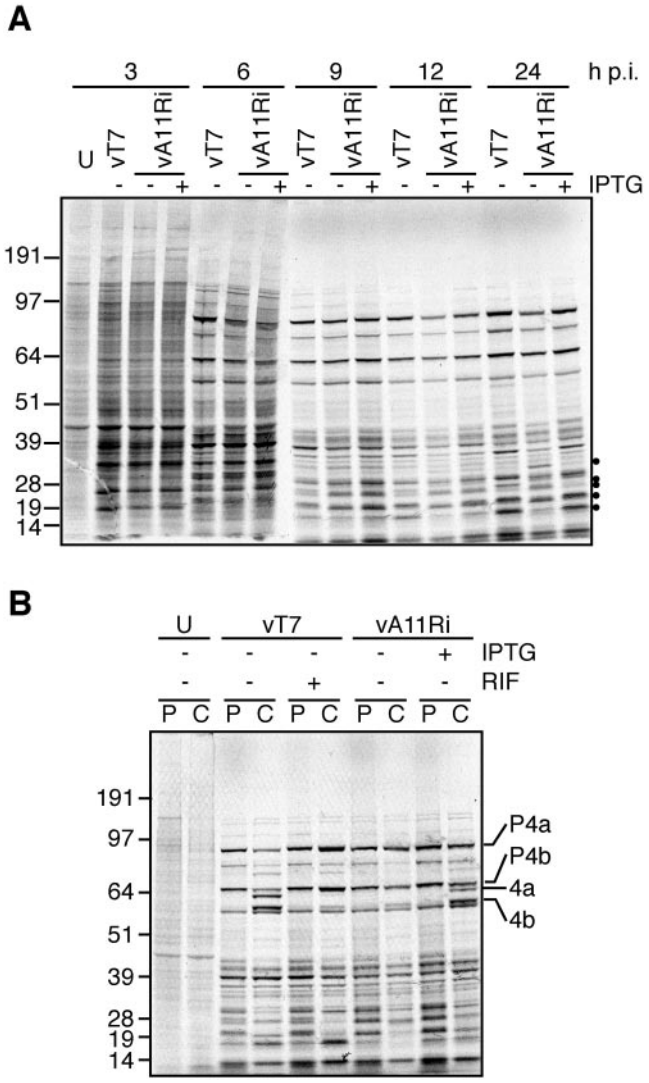

FIG. 6. Synthesis and processing of viral proteins. (A) Pulse-labeling of synthesized proteins. BS-C-1 cells were infected with vT7lacOI or vA11Ri in the absence or presence of 25 μM IPTG at a multiplicity of 5 PFU per cell. Infected cells were labeled with [^{35}S]methionine and [^{35}S]cysteine for 30 min at 3 to 24 h postinfection (h p.i.), whole-cell lysates were prepared, and proteins were separated by SDS-PAGE, followed by autoradiographic visualization. Uninfected cells (U) were similarly labeled to differentiate viral from cellular proteins. Migration and mass in kilodaltons of marker proteins are indicated on the left. Note that several proteins indicated by filled circles on the right are synthesized at rates that differ between the three conditions. (B) Proteolytic processing of core proteins. BS-C-1 cells were infected with vT7lacOI in the absence or presence of 100 μg of rifampin(RIF)/ml or with vA11Ri in the absence or presence of 25 μM IPTG at a multiplicity of infection of 5 PFU per cell. Uninfected cells (U) were used as a control. After pulse-labeling at 9 h, the cells were either harvested directly (P) or shifted into chase media (C) containing excess unlabeled amino acids for 14 h before harvest. Proteins in whole-cell extracts of harvested cells were separated by SDS-PAGE and visualized by autoradiography. Major core protein precursors (P4a and P4b) and their mature processed products (4a and 4b) are indicated on the right. Position and mass in kilodaltons of marker proteins are shown on the left.

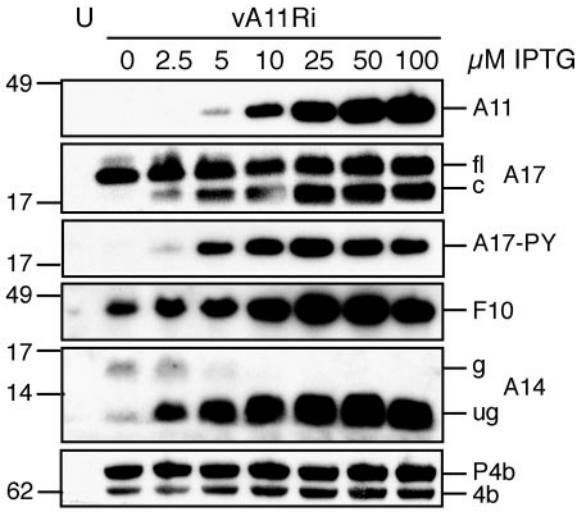

FIG. 7. Effects of A11 repression on proteins involved in early morphogenesis. BS-C-1 cells were infected with 10 PFU per cell of vA11Ri in the presence of the indicated concentrations of IPTG. After 24 h, whole-cell extracts were prepared, fractionated by SDS-PAGE, and analyzed by Western blotting with anti-A11, anti-A17-N (detecting full-length [fl] and proteolytically cleaved [c] forms of A17), anti-pTyr (A17-PY), anti-F10, anti-A14-C (detecting glycosylated [g] and unglycosylated [ug] forms of A14) and anti-P4b/4b antisera. Loading of similar amounts of extract was verified by the detection of similar levels of P4b.

the relevance of this interaction was not determined. Also unclear was the relevance and function of the phosphorylation of A11 described here. Unexpectedly, A11 was phosphorylated in the absence of the F10 protein kinase, which plays an important role in early stages of virogenesis. F10 overexpression did, however, increase the phosphorylation of A11. It is as yet unclear which kinase phosphorylates A11 in the absence of F10. A possible candidate would be the VAC B1 kinase. Although some VAC B1 temperature-sensitive mutants have defects in DNA replication (25) and intermediate gene expression (18) at the nonpermissive temperature, at least one has been described as synthesizing normal amounts of DNA but having aberrant morphogenesis, although the arrest is at the stage of IVs (9, 19).

Despite some minor differences, viral late protein synthesis and reduction of host protein synthesis were largely unaffected by the absence of A11. On the other hand, the proteolytic processing of several late proteins, including P4a and P4b, was severely inhibited in the absence of A11. The inhibition of protein processing is typically observed when morphogenesis is blocked at or before the IV stage. We therefore examined the expression and posttranslational modification of several proteins that are affected by early morphogenesis blocks. The A17 protein was found to be neither cleaved nor phosphorylated when A11 was suppressed. Since A17 cleavage likely occurs before the formation of membrane crescents (3, 28), we concluded that in the absence of A11 virogenesis might be blocked before the formation of normal viral membrane structures. The expression level of the F10 kinase, which is responsible for the phosphorylation of A17, was modestly reduced without A11, but the reduction may not be sufficient to account for the complete absence of A17 phosphorylation. Also consis-

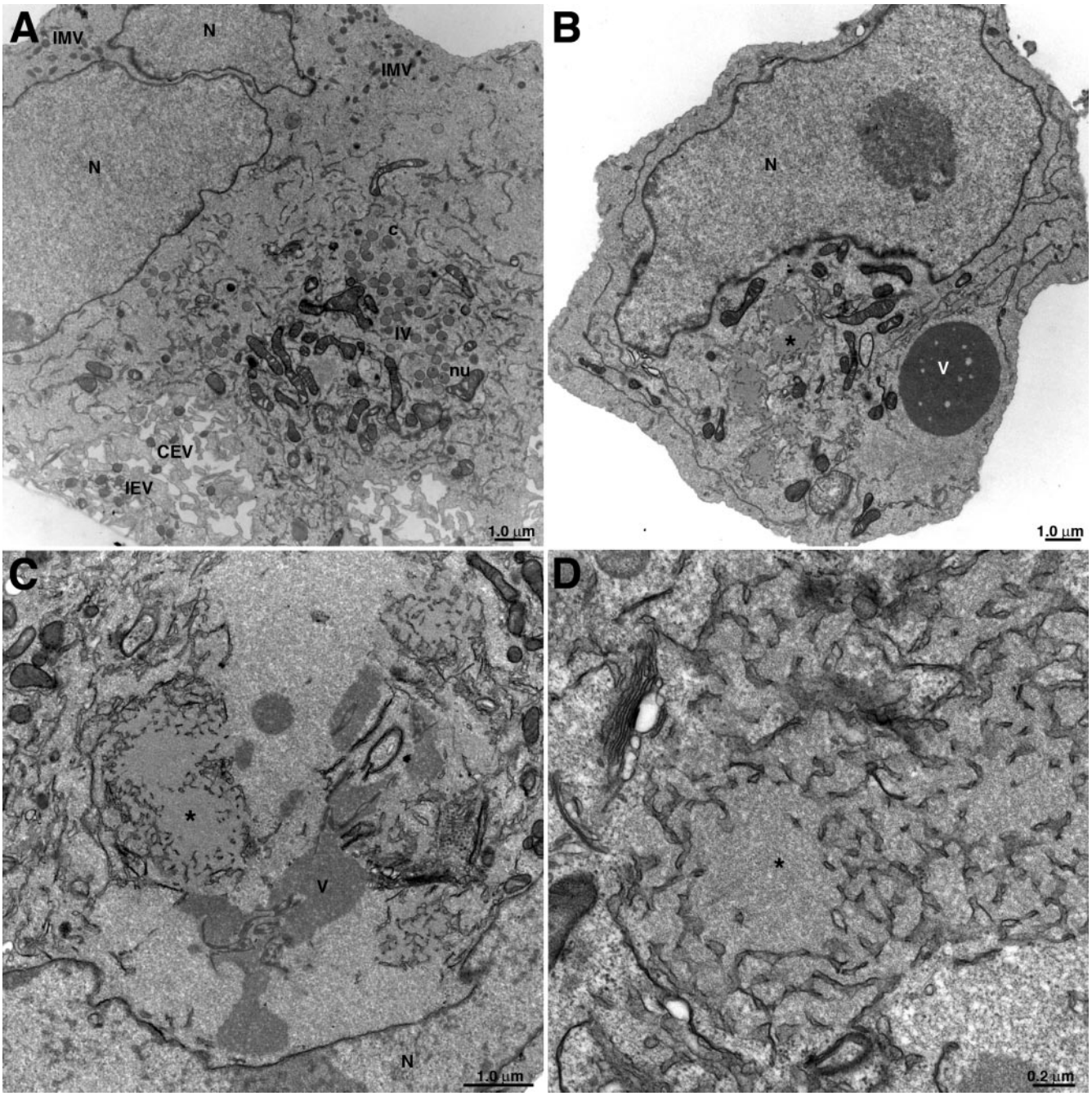

FIG. 8. Electron microscopy of infected cells. BS-C-1 cells were infected with 3 PFU per cell of vA11Ri in the presence (A) or absence (B to D) of 25 μM IPTG. Cells were fixed and prepared for transmission electron microscopy at 20 h after infection. Electron micrographs are shown with their scale indicated by the bars. Abbreviations: c, crescent; IV, immature virion; nu, nucleoid within an IV; IMV, intracellular mature virion; IEV, intracellular enveloped virion; CEV, cell-associated enveloped virion; V, viroplasm; ❋, intermediate density area; N, nucleus.

tent with a very early interruption of morphogenesis was the inappropriate glycosylation of A14. This glycosylation event also occurs in the absence of functional H5, F10, or A17 (21), suggesting that A11 may act at a step similar to these proteins. We noted, however, that in our experiments a larger fraction of A14 was glycosylated, although we cannot exclude that glycosylation might have interfered with antibody binding in the previous report, leading to a lower estimate for the amount of glycosylated A14.

Electron microscopy of cells infected with vA11Ri in the absence of IPTG showed a striking defect in morphogenesis, as predicted from the protein processing results. In the cytoplasm large, clear areas that excluded cellular organelles contained dense, granular masses of viroplasm. Similar to infections in the absence of functional A30 (37), A14 (30), and F10 (35), the masses of viroplasm were demarcated by sharp boundaries without the presence of any surrounding membranes. Similar masses were also seen in infections in the presence of rifampin

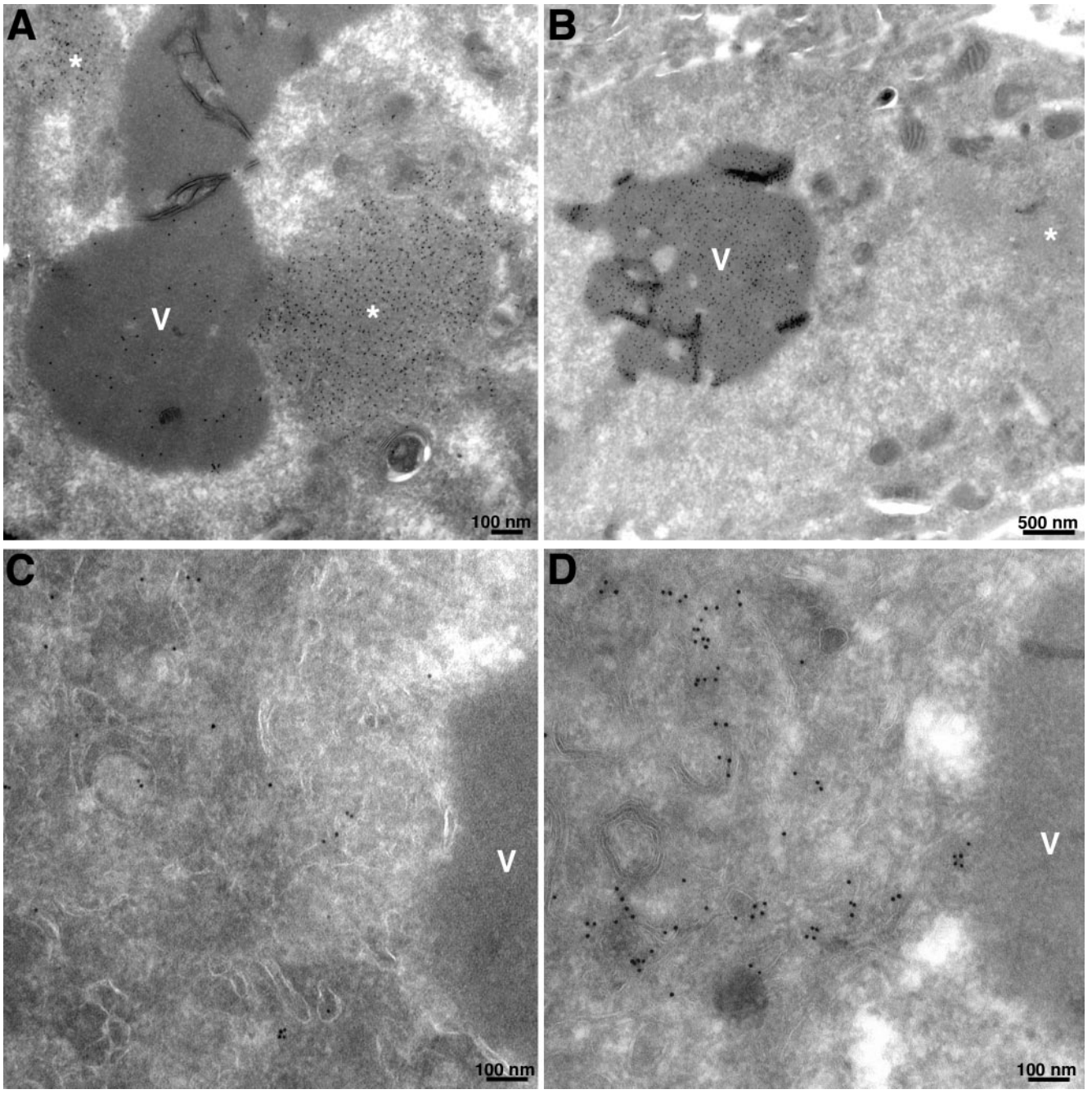

FIG. 9. Localization of A17, A3 (P4b), D13, and PDI by immunoelectron microscopy. Cells were infected with 3 PFU per cell of vA11Ri in the absence of IPTG. After 24 h, cells were fixed, cryosectioned, and incubated with anti-D13 (A), anti-P4b/4b (B), anti-A17-N (C), or anti-PDI antisera (D), followed by an appropriate secondary antibody and colloidal gold coupled to protein A. Electron micrographs are shown with scale bars. Abbreviations: V, viroplasm; ✻, intermediate density area.

(24) or in the absence of A17 (27), but in both cases membranes were associated with the dense viroplasm, either as sheets or as vesicles and tubules. The viroplasm masses seen here were also distinct from those observed in the temperature-sensitive mutants of two other genes that are involved in the early steps of membrane crescent formation, namely, H5R (12) and G5R (7). In these mutants lace doily-like structures were found at the elevated temperature and are referred to as curdled virosomes. In addition to the viroplasm masses, we also observed areas of intermediate electron density that were associated with membrane structures and were found inside and outside of the viral factories. The texture of these areas was reminiscent of D13 inclusion bodies that formed in the presence of rifampin (33). D13 is thought to form the scaffold that confers the regular curvature upon the crescent and IV membranes (10, 15, 22). We confirmed that these intermediate-density areas did contain D13 by electron microscopy of thawed cryosections labeled with anti-D13 antibody and pro-

tein A coupled to colloidal gold and that these areas were distinct from the electron-dense viroplasm, which contained the majority of the P4b found in the infected cells. We detected low amounts of the IMV membrane protein A17 and the cellular ER-resident PDI associated with the membranes in the intermediate-electron-density regions. Since the two proteins were localized in separate samples, we could not draw firm conclusions about their presence in the same membrane structures. If, however, they did colocalize to these membranes, two models could explain the observation. First, these membranes could be bona fide precursors of viral membranes, derived from the ER. In this model, D13 would interact with these membranes inappropriately, perhaps prematurely, resulting in a dead-end product and thereby arresting morphogenesis. The suppression of A11 could cause this interaction if it was involved in regulating D13 interaction with a putative viral membrane anchor in the membrane precursors. Alternatively, A11 might arrest morphogenesis by some other mechanism, resulting in the inappropriate insertion of viral membrane proteins into the ER, causing as a secondary effect the accumulation of D13 and the association of the ER membranes with the intermediate-density areas. This would be consistent with inappropriate A14 glycosylation. If this interpretation was correct, we would expect to find such intermediate-electron-density areas consisting of D13 and membranes in other mutants with early blocks in morphogenesis. In addition to the distinct phenotype, A11 is also distinguished from the other late proteins required for viral membrane formation by its absence from IVs and IMVs.

ACKNOWLEDGMENTS

A. Garcia provided the pcDNA-A32HA plasmid. We thank N. Cooper for cell culture assistance.

REFERENCES

1. **Alexander, W. A., B. Moss, and T. R. Fuerst**. 1992. Regulated expression of foreign genes in vaccinia virus under the control of bacteriophage T7 RNA polymerase and the *Escherichia coli lac* repressor. J. Virol. **66:**2934–2942.
2. **Ansarah-Sobrinho, C., and B. Moss**. 2004. Role of the I7 protein in proteolytic processing of vaccinia virus membrane and core components. J. Virol. **78:**6335–6343.
3. **Betakova, T., E. J. Wolffe, and B. Moss**. 1999. Regulation of vaccinia virus morphogenesis: phosphorylation of the A14L and A17L membrane proteins and C-terminal truncation of the A17L protein are dependent on the F10L protein kinase. J. Virol. **73:**3534–3543.
4. **Byrd, C. M., T. C. Bolken, and D. E. Hruby**. 2002. The vaccinia virus I7L gene product is the core protein proteinase. J. Virol. **76:**8973–8976.
5. **Cassetti, M. C., M. Merchlinsky, E. J. Wolffe, A. S. Weisberg, and B. Moss**. 1998. DNA packaging mutant: repression of the vaccinia virus A32 gene results in noninfectious, DNA-deficient, spherical, enveloped particles. J. Virol. **72:**5769–5780.
6. **da Fonseca, F. G., A. Weisberg, E. J. Wolffe, and B. Moss**. 2000. Characterization of the vaccinia virus H3L envelope protein: topology and posttranslational membrane insertion via the C-terminal hydrophobic tail. J. Virol. **74:**7508–7517.
7. **da Fonseca, F. G., A. S. Weisberg, M. F. Caeiro, and B. Moss**. 2004. Vaccinia virus mutants with alanine substitutions in the conserved G5R gene fail to initiate morphogenesis at the nonpermissive temperature. J. Virol. **78:**10238–10248.
8. **da Fonseca, F. G., E. J. Wolffe, A. Weisberg, and B. Moss**. 2000. Effects of deletion or stringent repression of the H3L envelope gene on vaccinia virus replication. J. Virol. **74:**7518–7528.
9. **Dales, S., V. Milovanovitch, B. G. T. Pogo, S. B. Weintraub, T. Huima, S. Wilton, and G. McFadden**. 1978. Biogenesis of vaccinia: isolation of conditional lethal mutants and electron microscopic characterization of their phenotypically expressed defects. Virology **84:**403–428.
10. **Dales, S., and E. H. Mosbach**. 1968. Vaccinia as a model for membrane biogenesis. Virology **35:**564–583.
11. **Dales, S., and B. G. T. Pogo**. 1981. Biology of poxviruses, vol. 18. Springer-Verlag, New York, N.Y.
12. **DeMasi, J., and P. Traktman**. 2000. Clustered charge-to-alanine mutagenesis of the vaccinia virus H5 gene: isolation of a dominant, temperature-sensitive mutant with a profound defect in morphogenesis. J. Virol. **74:**2393–2405.
13. **Dubochet, J., M. Adrian, K. Richter, J. Garces, and R. Wittek**. 1994. Structure of intracellular mature vaccine virus observed by cryoelectron microscopy. J. Virol. **68:**1935–1941.
14. **Earl, P. L., B. Moss, L. S. Wyatt, and M. W. Carroll**. 1998. Generation of recombinant vaccinia viruses, p. 16.17.1–16.17.19. *In* F. M. Ausubel, R. Brent, R. E. Kingston, D. D. Moore, J. G. Seidman, J. A. Smith, and K. Struhl (ed.), Current protocols in molecular biology, vol. 2. Greene Publishing Associates & Wiley Interscience, New York, N.Y.
15. **Grimley, P. M., E. N. Rosenblum, S. J. Mims, and B. Moss**. 1970. Interruption by rifampin of an early stage in vaccinia virus morphogenesis: accumulation of membranes which are precursors of virus envelopes. J. Virol. **6:**519–533.
16. **Hollinshead, M., A. Vanderplasschen, G. L. Smith, and D. J. Vaux**. 1999. Vaccinia virus intracellular mature virions contain only one lipid membrane. J. Virol. **73:**1503–1517.
17. **Katz, E., and B. Moss**. 1970. Formation of a vaccinia virus structural polypeptide from a higher molecular weight precursor: inhibition by rifampicin. Proc. Natl. Acad. Sci. USA **6:**677–684.
18. **Kovacs, G. R., N. Vasilakis, and B. Moss**. 2001. Regulation of viral intermediate gene expression by the vaccinia virus B1 protein kinase. J. Virol. **75:**4048–4055.
19. **Lackner, C. A., S. M. D'Costa, C. Buck, and R. C. Condit**. 2003. Complementation analysis of the Dales collection of vaccinia virus temperature-sensitive mutants. Virology **305:**240–259.
20. **McCraith, S., T. Holtzman, B. Moss, and S. Fields**. 2000. Genome-wide analysis of vaccinia virus protein-protein interactions. Proc. Natl. Acad. Sci. USA **97:**4879–4884.
21. **Mercer, J., and P. Traktman**. 2003. Investigation of structural and functional motifs within the vaccinia virus A14 phosphoprotein, an essential component of the virion membrane. J. Virol. **77:**8857–8871.
22. **Mohandas, A. R., and S. Dales**. 1995. Involvement of spicules in the formation of vaccinia virus envelopes elucidated by a conditional lethal mutant. Virology **214:**494–502.
23. **Moss, B**. 2001. Poxviridae: the viruses and their replication, p. 2849–2883. *In* D. M. Knipe and P. M. Howley (ed.), Fields virology, 4th ed., vol. 2. Lippincott/The Williams & Wilkins Co., Philadelphia, Pa.
24. **Moss, B., E. N. Rosenblum, E. Katz, and P. M. Grimley**. 1969. Rifampicin: a specific inhibitor of vaccinia virus assembly. Nature **224:**1280–1284.
25. **Rempel, R. E., and P. Traktman**. 1992. Vaccinia virus-B1 kinase: phenotypic analysis of temperature-sensitive mutants and enzymatic characterization of recombinant proteins. J. Virol. **66:**4413–4426.
26. **Risco, C., J. R. Rodriguez, C. Lopez-Iglesias, J. L. Carrascosa, M. Esteban, and D. Rodriguez**. 2002. Endoplasmic reticulum-Golgi intermediate compartment membranes and vimentin filaments participate in vaccinia virus assembly. J. Virol. **76:**1839–1855.
27. **Rodríguez, D., M. Esteban, and J. R. Rodríguez**. 1995. Vaccinia virus A17L gene product is essential for an early step in virion morphogenesis. J. Virol. **69:**4640–4648.
28. **Rodriguez, D., J. R. Rodriguez, and M. Esteban**. 1993. The vaccinia virus 14-kilodalton fusion protein forms a stable complex with the processed protein encoded by the vaccinia virus A17L gene. J. Virol. **67:**3435–3440.
29. **Rodriguez, J. R., C. Risco, J. L. Carrascosa, M. Esteban, and D. Rodriguez**. 1997. Characterization of early stages in vaccinia virus membrane biogenesis: implications of the 21-kilodalton protein and a newly identified 15-kilodalton envelope protein. J. Virol. **71:**1821–1833.
30. **Rodriguez, J. R., C. Risco, J. L. Carrascosa, M. Esteban, and D. Rodriguez**. 1998. Vaccinia virus 15-kilodalton (A14L) protein is essential for assembly and attachment of viral crescents to virosomes. J. Virol. **72:**1287–1296.
31. **Smith, G. L., A. Vanderplasschen, and M. Law**. 2002. The formation and function of extracellular enveloped vaccinia virus. J. Gen. Virol. **83:**2915–2931.
32. **Sodeik, B., R. W. Doms, M. Ericsson, G. Hiller, C. E. Machamer, W. van't Hof, G. van Meer, B. Moss, and G. Griffiths**. 1993. Assembly of vaccinia virus: role of the intermediate compartment between the endoplasmic reticulum and the Golgi stacks. J. Cell Biol. **121:**521–541.
33. **Sodeik, B., G. Griffiths, M. Ericsson, B. Moss, and R. W. Doms**. 1994. Assembly of vaccinia virus: effects of rifampin on the intracellular distribution of viral protein p65. J. Virol. **68:**1103–1114.
34. **Sodeik, B., and J. Krijnse-Locker**. 2002. Assembly of vaccinia virus revisited: de novo membrane synthesis or acquisition from the host? Trends Microbiol. **10:**15–24.
35. **Szajner, P., A. S. Weisberg, and B. Moss**. 2004. Evidence for an essential catalytic role of the F10 protein kinase in vaccinia virus morphogenesis. J. Virol. **78:**257–265.
36. **Szajner, P., A. S. Weisberg, and B. Moss**. 2004. Physical and functional interactions between vaccinia virus F10 protein kinase and virion assembly proteins A30 and G7. J. Virol. **78:**266–274.
37. **Szajner, P., A. S. Weisberg, E. J. Wolffe, and B. Moss**. 2001. Vaccinia virus

A30L protein is required for association of viral membranes with dense viroplasm to form immature virions. J. Virol. **75:**5752–5761.
38. **Traktman, P., A. Caligiuri, S. A. Jesty, and U. Sankar**. 1995. Temperature-sensitive mutants with lesions in the vaccinia virus F10 kinase undergo arrest at the earliest stage of morphogenesis. J. Virol. **69:**6581–6587.
39. **Traktman, P., K. Liu, J. DeMasi, R. Rollins, S. Jesty, and B. Unger**. 2000. Elucidating the essential role of the A14 phosphoprotein in vaccinia virus morphogenesis: construction and characterization of a tetracycline-inducible recombinant. J. Virol. **74:**3682–3695.
40. **Upton, C., S. Slack, A. L. Hunter, A. Ehlers, and R. L. Roper**. 2003. Poxvirus orthologous clusters: toward defining the minimum essential poxvirus genome. J. Virol. **77:**7590–7600.
41. **Wang, S., and S. Shuman**. 1995. Vaccinia virus morphogenesis is blocked by temperature-sensitive mutations in the F10 gene, which encodes protein kinase 2. J. Virol. **69:**6376–6388.
42. **Ward, G. A., C. K. Stover, B. Moss, and T. R. Fuerst**. 1995. Stringent chemical and thermal regulation of recombinant gene expression by vaccinia virus vectors in mammalian cells. Proc. Natl. Acad. Sci. USA **92:**6773–6777.
43. **Wolffe, E. J., D. M. Moore, P. J. Peters, and B. Moss**. 1996. Vaccinia virus A17L open reading frame encodes an essential component of nascent viral membranes that is required to initiate morphogenesis. J. Virol. **70:**2797–2808.
44. **Zhang, Y., and B. Moss**. 1992. Immature viral envelope formation is interrupted at the same stage by lac operator-mediated repression of the vaccinia virus D13L gene and by the drug rifampicin. Virology **187:**643–653.